Molecular Dynamics Study of the Dopamine D2 Receptor Bound to Eticlopride and Two Derivative Molecules

SAMUEL ESCUDERO, ALEXIOS GIANNOULAS, XARENI REYES SOTO.

KEYWORDS: GPCR, DOPAMINE, D2R RECEPTOR, MOLECULAR DYNAMICS

INTRODUCTION. A significant proportion of the drugs in the market target a specific family of proteins known as G protein coupled receptors (GPCRs). This paper focuses on the dopamine D2 receptor (D2R). This is a GPCR that plays a critical role in modulating cognitive function, motivation, reward, and movement through its interaction with the neurotransmitter dopamine (O Klein et*al*., 2016).

Eticlopride (ETQ) is a high affinity antagonist of the dopamine D2 receptor (D2R), a G protein coupled receptor (GPCR) that modulates dopaminergic signaling in the central nervous system. Widely expressed in pathways linked to motivation, reward, and motor control, the D2R is a crucial target for pharmacological interventions, particularly in the treatment of psychiatric and neurological disorders (Missale *etal.,* 1998).

In this work, we focus on the dopamine D2 receptor (D2R) and its interactions with the antagonist eticlopride (ETQ) by studying its PDB structure (PDB ID: 3PBL Chien *et al.,* 2010) and exploring two newly designed derivatives. Based on the insights obtained from the original 3PBL D2R complex, we introduced specific chemical modifications to ETQ to improve its binding properties. Using molecular dynamics simulations, our goal is to evaluate how these alterations affect the ligand receptor interactions and to advance drug discovery efforts by providing a framework for the rational design of optimized compounds targeting D2R.

RESULT & DISCUSSION.

In the first derivative (ETQF), the chlorine atom of ETQ is replaced by fluorine, while in the second (ETQA), an additional carbon with a double bond (C=C) is introduced at the C15 (***Figure 1***).

ETQF was designed to improve contacts found around the chloride atom of ETQ. Our team observed that the chloride atom of ETQ forms a hydrogen bond network with residues THR115, SER196, and CYS114, which stabilises the ligand binding to the receptor. The goal of changing the chloride atom with the more electronegative atom fluoride, is strengthening this hydrogen bond network, and especially improving contacts with residues CYS114 and SER196 (***Figure 2***).

ETQA was designed to improve contacts found in the outer part of the protein, strengthening the hydrophobic interactions with its surrounding residues, while displacing water.

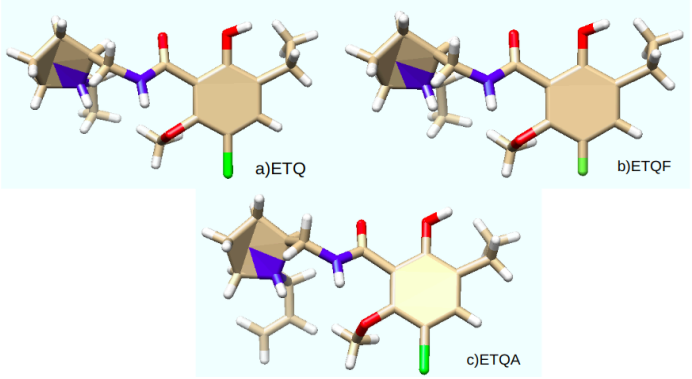

Figure 1. Comparison of the ligand antagonist ETQ, and its two derivatives ETQF and ETQA.

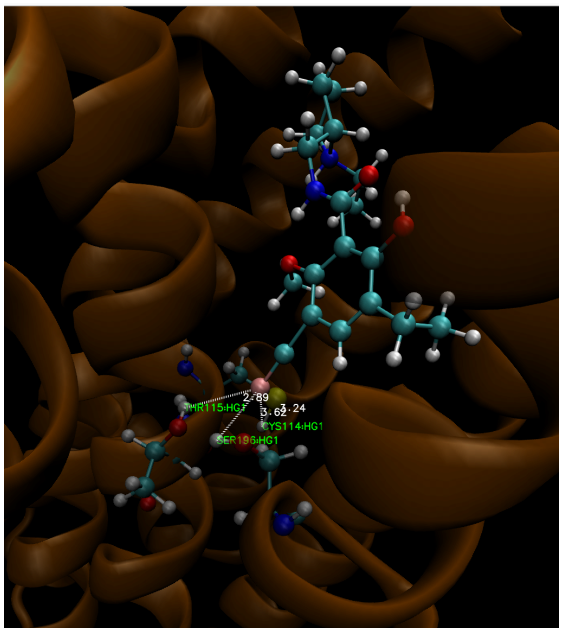

Figure 2. Hydrogen bond network formed by the chloride of ETQ and residues THR115, SER196, and CYS114 of the receptor D2R.

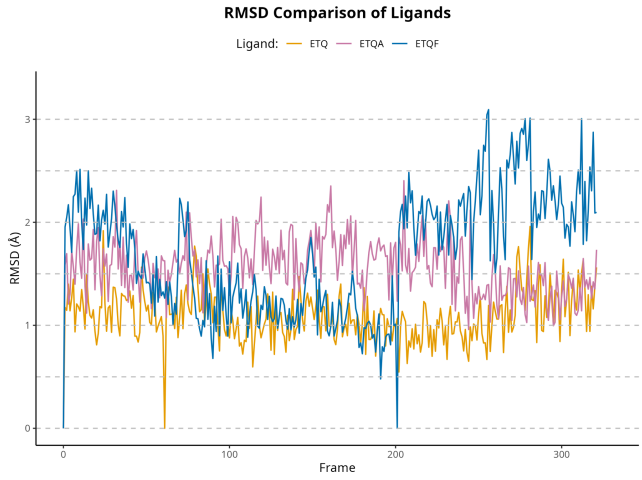

Figure 3. RMSD comparison for ETQ, and its two derivatives ETQF and ETQA.

The root-mean-square deviation (RMSD) was plotted for all three ligands to evaluate their stability over the course of the simulation (Figure 3). All ligands exhibited relatively low RMSD values overall (below 3 Å), indicating stable binding to the receptor. The RMSD plot for ligand ETQA showed greater fluctuations compared to the other two ligands, which can be attributed to the added flexibility introduced by the alkene group modification. With access to improved computational resources, a longer production run could be conducted to allow a more comprehensive exploration of binding conformations over time.

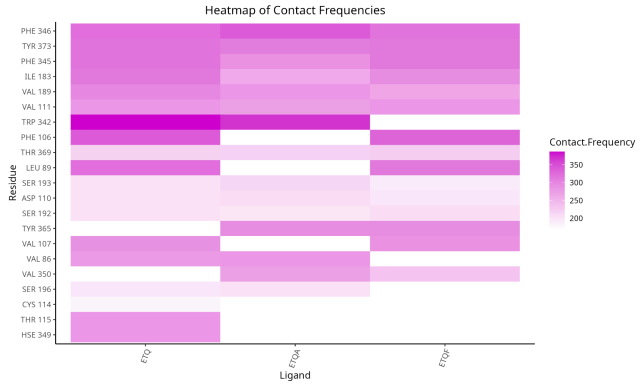

Figure 4. Contact frequencies for ETQ, and its two derivatives ETQF and ETQA.

To better understand the molecular interactions between each ligand and the receptor, interselection contacts were calculated throughout the simulation. This analysis identifies which residues from the receptor remain in close proximity over time with the ligand, providing insights into the stability and specificity of the binding.

Comparing ligand ETQ and ETQF (***Figure 4***) 6 contacts are lost (VAL86, CYS114, THR115, SER196, TRP342, HSE349), while 2 new contacts are formed (VAL350, TYR365). It is evident that the contacts that were expected to improve in the hydrogen bond network (THR115, SER196, and CYS114) are being lost. The reason is that when a halogen is introduced into a molecule, a dummy atom must be put in place, in order for the electrostatic terms to be realistic. In the case of ETQF, a dummy atom was not introduced for the fluoride, and the stabilization of the bottom part of the ligand is altered due to the loss of the hydrogen bond network. Interactions with residues VAL350, TYR365, which are on the part of the ligand that faces the extracellular part of the receptor, are probably formed due to the loss of binding in the bottom part of the ligand that was explained above, which allows freedom of movement towards them.

Comparing ligand ETQ and ETQA (***Figure 4***) 5 contacts are lost (LEU89, PHE106, VAL107, THR115, HSE349), while 2 new contacts are formed (VAL350, TYR365), and 1 contact was improved (PHE 346). This can be explained by the fact that the newly formed contacts together with the improved contact pull the ligand ETQA towards them and away from the residues where contacts were lost (***Figure 5***).

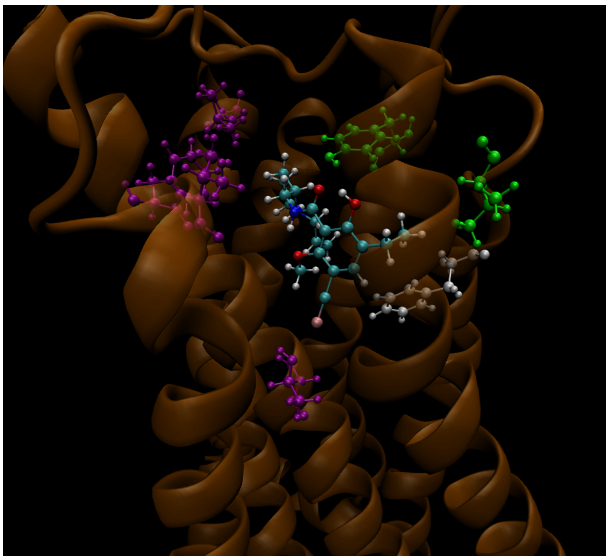

Figure 5. Ligand ETQA shown together with residues were contacts were lost (magenta), residues where contacts were formed (green), and where contact was improved (white).

Overall, the number of contacts was not significantly improved for either of the two new ligands (Figure 6). In the case of ligand ETQA, the modification was likely not effective enough to enhance overall interactions. However, for ETQF, the situation is less clear. Re-running the simulation for ETQF with corrected electrostatic parameters for the fluoride atom could help determine whether the halogen's electronegativity plays a significant role in the binding of ETQ ligands to the D2R receptor.

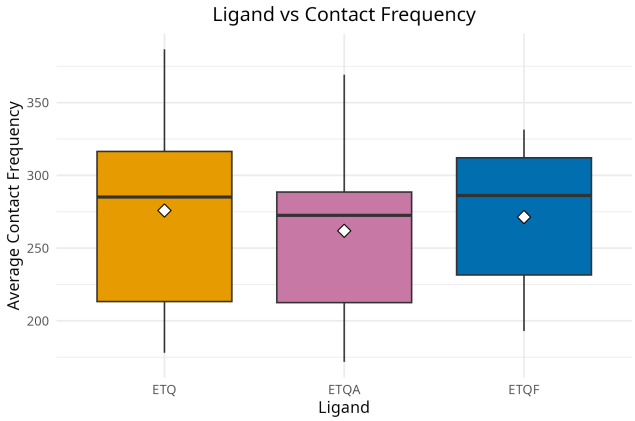

Figure 6. Comparison of ligand and contact frequency for ETQ, and its two derivatives ETQF and ETQA. The mean of the contact frequencies of each ligand is shown as a white square.

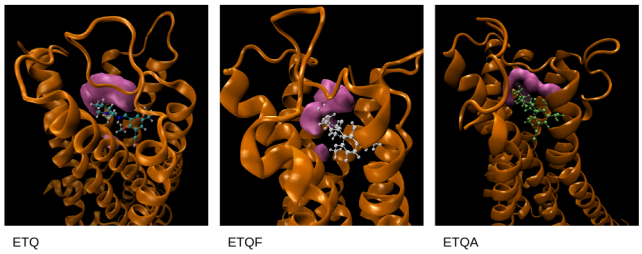

Figure 7. Water Volmap for the ligand ETQ, and its two derivatives ETQF and ETQA.

The water density maps (Volmap) (***Figure 7***) reveal differences in solvent distribution around the binding site for the three ligands. For ETQ, a well defined high density water region is observed within the binding pocket, suggesting strong solvent interactions and stabilization. In contrast, ETQF and ETQA show a more diffuse and less concentrated water distribution, which may indicate altered ligand positioning or reduced solvent mediated stabilization. These variations could reflect differences in binding affinity or dynamic behavior of each ligand within the receptor.

Steered Molecular Dynamics Analysis

Steered molecular dynamics (SMD) analysis was only feasible for ETQF, as the presence of a dummy atom in ETQ and ETQA introduced a lone pair of electrons with unknown parameters, prohibiting the namd equilibration to begin. All necessary equilibration steps for ETQF were performed using both GROMACS and NAMD. For ETQ and ETQA, the simulations failed due to an error related to an unstable atom, likely associated with the presence of a chlorine atom in the original ligand structure.

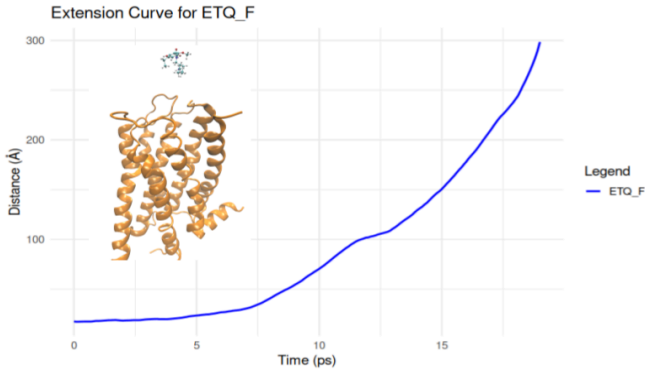

Figure 8. Extension curve for ETQF.

In **Figure 8**, the ETQF extension curve shows a progressive increase in distance throughout the targeted SMD. The ligand experiences small fluctuations as it moves away from the dopamine D2 receptor, suggesting that it overcomes small energetic barriers along the way. Overall, the final distance reached in the last frame is consistent with the traction velocity and configuration conditions, indicating that ETQF maintained stable interactions until later stages of the extension.

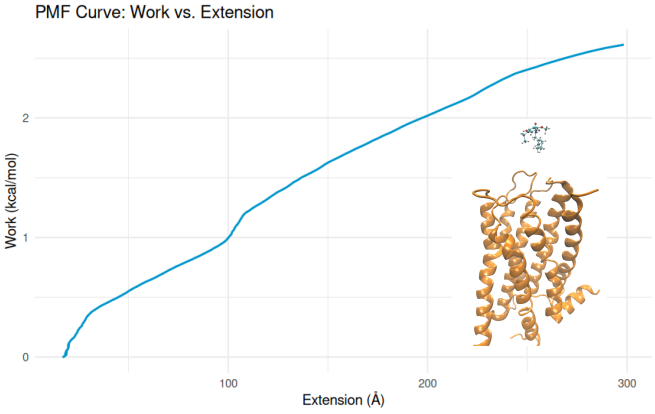

Figure 9. Potential of Mean Force for ETQF.

The mean force potential (PMF) curve in **Figure 9** reveals that the work required to separate ETQF from the receiver gradually increases with increasing extent. The initial slope of the curve is relatively shallow, implying that ETQF does not encounter a large free energy barrier at early distances. However, beyond a certain point, the work required increases more steeply, reflecting plausible interactions between the receptor and the ligand in the deeper pocket. These findings confirm that the fluorine modified ligand retains robust binding affinity, but can still be unbound with sufficient strength, providing useful information for further ligand optimization.

The initial goal of this analysis was the comparison of the PMF of the 3 ligands, aiming to discover whether the modifications made the affinity of the ligands stronger or not. A higher PMF would suggest that more force is

required to move the ligand away from the receptor, and therefore a better binding affinity, while a lower PMF would suggest the opposite.

CONCLUSION.

Our study explored the improvement of ligand binding properties at the dopamine D2 receptor through molecular dynamics simulations and steered MD experiments. We investigated eticlopride (ETQ) and its derivatives, ETQF and ETQA, designed via chemical modifications aimed at enhancing binding affinity and unbinding dynamics.

Following a standard molecular dynamics simulation workflow, we plotted the RMSD for all ligands and highlighted the need for longer production runs to better explore potential conformational changes.

Additionally, the contacts between each ligand and the D2 receptor were analyzed, with residue-level differences visualized using a heatmap and overall interaction trends represented through boxplots. This part of the analysis demonstrated the complexity of improving ligand binding and emphasized the need for enhanced computational tools to accurately model halogen electrostatic interactions.

Although we were unable to complete the steered MD simulations for the original ETQ and ETQA, the results from the ETQF simulation provided valuable insights. The extension and potential of mean force (PMF) analyses revealed that substituting chlorine with fluorine in ETQF maintained stable ligand-receptor interactions while allowing for effective unbinding under force.

In this final part of the study, we again highlighted the need for better representation of halogen electrostatic interactions, as current computational methods do not accurately capture the behavior of halogenated compounds. These findings underscore the potential of strategic chemical modifications in drug discovery and lay the groundwork for future optimization of ligand binding to the D2 receptor.

METHODS.

The preparation of systems for the three ligands followed a similar protocol.

The original PDB file for the complex 3PBL-D2R (PDB ID: 3PBL) was obtained from the Protein Data Bank (Chien *et al.,* 2010). This PDB file was modified as follows: selected chain A to include residues 26-231, and chain B to include residues 313-400. A MOL2 file for eticlopride (ETQ) was generated using UCSF Chimera.

The two derivatives ETQF and ETQA were created using Chimera.

The cleaned PDB structure and ETQ MOL2 file were used as inputs for CHARMM-GUI's Membrane Builder tool (Brooks *et al.*, 2009; Jo *et al.*, 2008; Lee et *al.*, 2016; Wu et *al.*, 2016). Two disulfide bonds, between CYS103-CYS181 and CYS355-CYS358 were identified and specified in CHARMM GUI. The system was solvated and ionized to a concentration of 150 mM NaCl. The membrane was composed of POPC lipids. Input files for both GROMACS (Bekker et *al.*, 1993) and NAMD (Phillips *et al.,* 2020) were generated; the GROMACS files were used for system equilibration.

Following system assembly, energy minimization was performed, followed by a six step equilibration protocol. Production runs were conducted using three replicates of 2 ns and one replicate of 20 ns, resulting in 322 frames after concatenation.

The resulting .gro and .xtc files were analyzed in VMD (Humphrey *et al.,* 1996) to calculate the root-mean-square deviation (RMSD) of the protein (excluding the ligand), the RMSD of the ligand itself, and the ligand-receptor interaction dynamics over time.The RMSD of the ligands were plotted together using R language with the package "ggplot2" (Wickham, 2016).

Interselect-contacts for ETQ were computed using the VMD Timeline tool with 4 Å as cutoff distance and selection "same residue as within 3 of resname ETQ". The data was saved to a .tml file and analyzed using a custom Python script. The contact frequencies were plotted using R. Contact frequency plots for ETQF and ETQA were obtained similarly.

The water VolMap for ETQ was created using the VMD VolMap Tool with the following parameters: selection "water within 3 of resname ETQ", occupancy as Volmap type and selected the append to molecule option. Water maps for the two derivatives were created equally.

The Steered Molecular Dynamics (SMD) simulations were carried out using NAMD 2.13 with input files generated via CHARMM GUI. The system was first equilibrated at 303.15 K using a Langevin thermostat to ensure thermal stability. A timestep of 2 fs was used, and periodic boundary conditions were applied with Particle Mesh Ewald (PME) for long-range electrostatics, using a grid spacing of 1.0 Å and a van der Waals cutoff of 12.0 Å.

During the production phase, a total of 50,000 steps (corresponding to 100 ps) were executed. A pulling force was applied along the positive z axis at a constant velocity of 0.002 Å per timestep, with a harmonic force constant of 7.2 kcal/mol. The ligand was progressively displaced while the receptor remained fixed, simulating a directional unbinding process. The system's coordinates were saved every 250 steps, resulting in a trajectory of 25 frames for analysis.

Our github repository contains the code and the data that were used for this study.

https://github.com/Sam-E18/MSI_project_D2R_ETQ_2025

ABBREVIATIONS

GPCR, G protein coupled receptors; MD, Molecular Dynamics; RMSD, root mean square deviation; SMD, Steered Molecular Dynamics.

REFERENCES

Bekker, H., Berendsen, H. J. C., Dijkstra, E. J., Achterop, S., Vondrumen, R. V., Vanderspoel, D., ... & Renardus, M. K. R. (1993). Gromacs a parallel computer for molecular dynamics simulations. In the 4th *international conference on computational physics* (PC 92) (pp. 252-256). World Scientific Publishing.

Brooks, B. R., Brooks III, C. L., Mackerell Jr, A. D., Nilsson, L., Petrella, R. J., Roux, B., ... & Karplus, M. (2009). CHARMM: the biomolecular simulation program. Journal of computational chemistry, 30(10), 1545-1614.

Chien, E. Y., Liu, W., Zhao, Q., Katritch, V., Won Han, G., Hanson, M. A., ... & Stevens, R. C. (2010). Structure of the human dopamine D3 receptor in complex with a D2/D3 selective antagonist. Science, 330(6007), 1091-1095.

Humphrey, W., Dalke, A., & Schulten, K. (1996). VMD: visual molecular dynamics. *Journal of molecular graphics*, *14*(1), 33-38.

Jo, S., Kim, T., Iyer, V. G., & Im, W. (2008). CHARMM-GUI: a web-based graphical user interface for CHARMM. Journal of computational chemistry, 29(11), 1859-1865.

Lee, J., Cheng, X., Jo, S., MacKerell, A. D., Klauda, J. B., & Im, W. (2016). CHARMM-GUI input generator for NAMD, GROMACS, AMBER, OpenMM, and CHARMM/OpenMM simulations using the CHARMM36 additive force field. *Biophysical journal*, *110*(3), 641a.

Missale, C., Nash, S. R., Robinson, S. W., Jaber, M., & Caron, M. G. (1998). Dopamine receptors: from structure to function. Physiological Reviews, 78(1), 189–225. https://doi.org/10.1152/physrev.1998.78.1.189

O Klein, M., Battagello, D. S., Cardoso, A. R., Hauser, D. N., Bittencourt, J. C., & Correa, R. G. (2016). Dopamine: functions, signaling, and association with neurological diseases. Cellular and molecular neurobiology, 39(1), 31-59.

Phillips, J. C., Hardy, D. J., Maia, J. D., Stone, J. E., Ribeiro, J. V., Bernardi, R. C., ... & Tajkhorshid, E. (2020). Scalable molecular dynamics on CPU and GPU architectures with NAMD. *The Journal of chemical physics*, 153(4).

Wickham, H. (2016). Data analysis. *ggplot2: Elegant graphics for data analysis*, 189-201.

Wu, E. L., Cheng, X., Jo, S., Rui, H., Song, K. C., Dávila-Contreras, E. M., ... & Im, W. (2014). CHARMM-GUI membrane builder toward realistic biological membrane simulations.